Good Vibrations: Locking of Octahedral Tilting in Mixed-Cation Iodide Perovskites for Solar Cells

Dibyajyoti Ghosh,[†] Philip Walsh Atkins,[‡] M. Saiful Islam,[*,‡] Alison Walker,[*,†] and Christopher Eames[‡]

[†]*Department of Physics, University of Bath, Bath BA2 7AY, UK*
[‡]*Department of Chemistry, University of Bath, Bath BA2 7AY, UK*

E-mail: m.s.islam@bath.ac.uk; a.b.walker@bath.ac.uk

ABSTRACT: Metal halide perovskite solar cells have rapidly emerged as leading contenders in photovoltaic technology. Compositions with a mixture of cation species on the A-site show the best performance and have higher stability. However, the underlying fundamentals of such an enhancement are not fully understood. Here, we investigate the local structures and dynamics of mixed A-cation compositions. We show that substitution of low concentrations of smaller cations on the A-site in formamidimium lead iodide ($CH(NH_2)_2PbI_3$) results in a global 'locking' of the PbI_6 octahedra tilting. In the locked structure the octahedra tilt at a larger angle but undergo a much reduced amplitude of rocking motion. A key impact of this feature is that the rotational or tumbling motion of the $CH(NH_2)_2^+$ molecular ion in a locked cage is severely restricted. We discuss the impact of locking on the photovoltaic performance and stability.

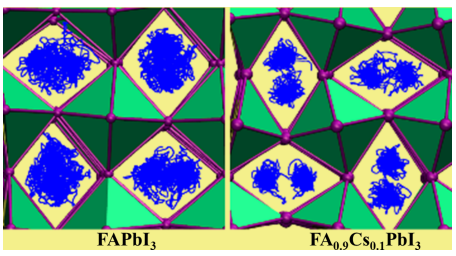

Metal halide perovskite solar cells have emerged[1–8] as a serious contender to silicon-based devices due to an unprecedented rise in power conversion efficiency, overtaking all other third-generation technologies. Despite their exceptional photovoltaic properties a number of challenges exist. Stability is a major concern: the archetypal phase $CH_3NH_3PbI_3$ ($MAPbI_3$) is thermodynamically unstable[9–11] and there are further significant problems associated with degradation in air and moisture.[12–15] There are also competing crystal phases that are not photoactive.[16,17] The presence of intrinsic defects at large concentrations also leads to ion transport[18,19] and current voltage hysteresis, as well as mediating degradation mechanisms.[14,20]

Improvement in the photovoltaic properties can be achieved by altering the composition.[21] Lead iodide perovskites have the general composition $APbI_3$ with the A-site occupied by a monovalent cation that can be organic or inorganic (A= methylammonium $CH_3NH_3^+$, formamidimium $CH(NH_2)_2^+$, caesium Cs^+ or rubidium Rb^+). As shown in Figure 1, the Pb/I component forms a framework of corner sharing octahedra with an A-site cation at the centre of each cage. Cation mixing on the A-site has been shown to significantly improve both the photovoltaic performance and the stability of these systems.[21–35] Typically, for mixed-cation perovskite studies, the host phase is formamidim-

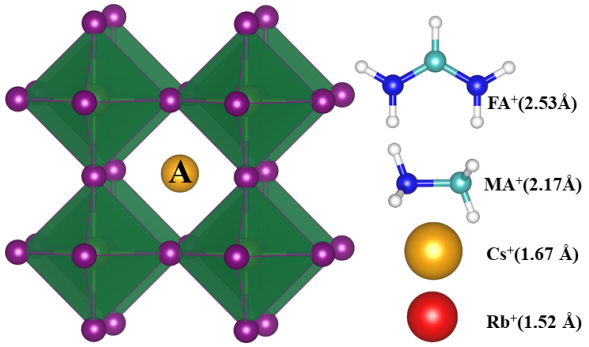

Figure 1: Structure of metal halide perovskite. 'A' cations (FA^+, MA^+, Cs^+ or Rb^+), shown on the right, occupy cages formed by corner-sharing PbI_6 octahedra. The ionic radii of these A-cations are given in brackets. Key: hydrogen (white), carbon (cyan), nitrogen (blue), iodine (pink).

ium lead iodide, $CH(NH_2)_2PbI_3$ ($FAPbI_3$) with small amounts of MA^+, Cs^+ and Rb^+ doped onto the A-site. The origin of the performance improvements upon such doping has been suggested as i) increased stability due to enhanced contribution from the entropy of mixing[30,36] ii) change of the Goldschmidt tolerance factor leading to altering of the tilting of the octahedra[37,38] and iii) reduction in crystal strain.[39]

However, lattice and A-site cation dynamics and their coupling have so far not been considered in detail, even though halide perovskites are found to be highly dynamical systems.[40–44] For example, in the related perovskite, $MAPbI_3$, the inorganic PbI_6 octahedral framework undergoes Glazer tilting with a time period of ∼0.2−1.5 picosecond (ps).[45] The FA^+ molecular ions on the A-site in $FAPbI_3$ undergo rotational or tumbling motion inside the cage (time period 2-3 ps[46]), and their internal bonds undergo dihedral rotation and vibration at a high frequency (time period 10-20 femtosecond (fs)[45]).

The impact of this considerable amount of motion upon the structure and properties of mixed A-cation perovskites, however, is not fully understood. Here, we use advanced *ab initio* molecular dynamics (AIMD) techniques (detailed in the SI) to investigate mixed A-cation perovskites based on $FAPbI_3$ substituted by MA^+, Cs^+ and Rb^+ to understand how their structures and dynamics compare to single A-cation phases.

First, we examine the effect on the perovskite structure upon cation substitution at the A-site of $FAPbI_3$. The volume per formula unit and mean Pb-I-Pb angle over time are shown in Figure 2. It can be seen that, when FA^+ is replaced by smaller cations, the cell-volume is reduced. For example, doping of 10% Rb^+ (smallest in size among the A-cations considered) causes a volume reduction of 2.2%. The effect is less pronounced when the intermediate sized cation MA^+ is involved. Doping of 10% MA^+ and 10% Cs^+ leads to a lower volume reduction of 0.8%. Details of equilibrium structural parameters of all mixed cation systems can be found in Table S1 in the SI.

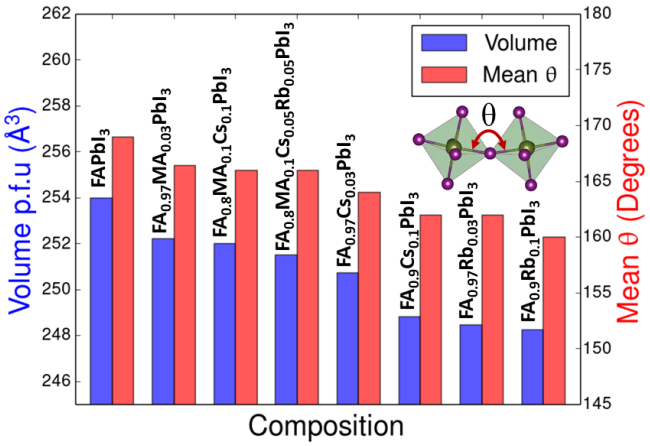

Figure 2: Dynamically averaged properties at 300K of lead iodide perovskites with various A-site compositions of $FAPbI_3$ doped with MA^+, Cs^+ and Rb^+. Equilibrium volume per formula unit (blue bars) and mean Pb-I-Pb angles over time (red bars). Inset shows the tilting of octahedrawith the octahedral tilting angle defined as the deviation in mean Pb-I-Pb angle from the ideal angle (180°) for a cubic phase.

The origin of this volume contraction is associated with the tilting of the PbI_6 corner-sharing octahedra. In the inset of Figure 2, we define the tilt angle between two corner sharing octahedra. Whilst the average crystal structure of $FAPbI_3$ is cubic,[46] locally the octahedra tilt to form an orthorhombic structure.[40,42] In our simulations, $FAPbI_3$ adopts such a tilted structure with an average tilt angle of 11° which

is very similar to the previous report.[42] We find that as smaller cations such as Cs^+ and/or Rb^+ are introduced onto the A-sites, they are less able to fill space in the cage, and as a result the octahedra tilt further to pack space more effectively. For example, the average tilt angle increases from 11° in $FAPbI_3$ to 20° in $FA_{0.9}Rb_{0.1}PbI_3$.

It is known that the hybrid perovskites are physically 'soft' and highly dynamical. With regard to lattice dynamics, the octahedra are found to undergo a rocking motion whereby the tilt angle of the corner sharing octahedra oscillates about the equilibrium position.[41,42,44,46–48] Here, we monitored this oscillatory motion for each composition, and the representative data as well as snapshots are displayed in Figure 3. We find a significant reduction in the amplitude of the rocking motion of octahedra for the mixed-cation phases. Focusing on a pair of octahedra (Figure 3b), the Pb-I-Pb angle in $FAPbI_3$ oscillates strongly over time in the range ≈ 135-180° (i.e. tilt angle of 0-45°) whereas the oscillation is restricted to a smaller range of ≈ 145-170° (i.e. tilt angle of 10-35°) for the Cs-doped system, $FA_{0.9}Cs_{0.1}PbI_3$.

The picture that emerges here is that when the parent $FAPbI_3$ is doped by smaller cations, the octahedra tilt at a greater angle. Furthermore, this tilting is 'locked' in place and undergoes much more restricted rocking dynamics (shown in Figure 3(b)). Following the Glazer notation,[49] time averaged geometries of these mixed cation systems exhibit locked 'in-phase tilting' (same-tilt) that is $a^0a^0c^+$ in the xy-crystal plane (see Figure S3 in SI for details). We note that previous AIMD studies by Quarti *et.al.* have demonstrated dynamics of $MAPbI_3$ where neighbouring octahedra undergo "out-of-phase"($a^0a^0c^-$) rotation by ± 30° along the c-axis in its tetrahedral phase.[42,44]

This 'locking' structural feature can be probed further using the radial distribution function (RDF). The Pb-I nearest-neighbour peak in $FAPbI_3$ at 3.18 Å remains unchanged upon doping (Figures S4 and S5 in SI), indicating that the internal geometry and bonding in the PbI_6 octahedra are unaltered by the increased tilting and do not contribute to the volume reduction.

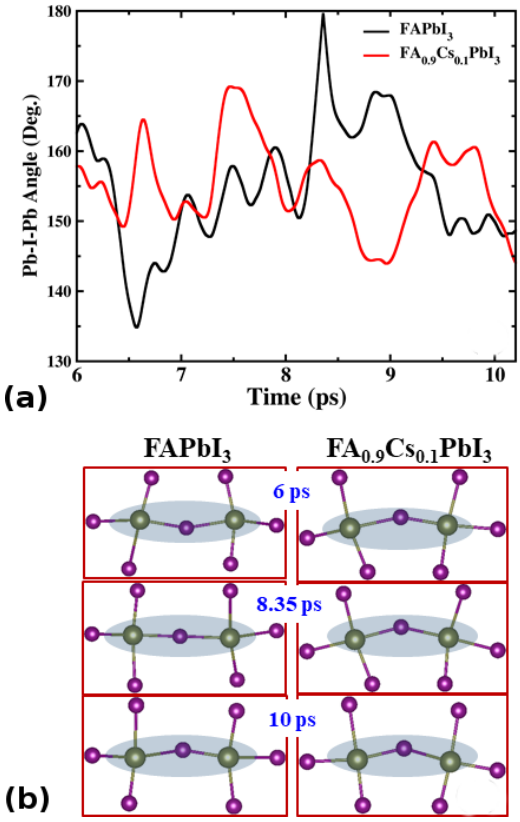

Figure 3: Octahedral motion of PbI_6 octahedra over time in pure $FAPbI_3$ and mixed-cation perovskites. (a) Variation in individual tilt angle with time in $FAPbI_3$ and $FA_{0.9}Cs_{0.1}PbI_3$, showing restricted tilting in the latter; (b) Snapshots of the tilting motion of those octahedra (shaded area) at different times. Periodic rocking motion of octahedra is only evident for the parent $FAPbI_3$.

We now consider the effects on bonding and molecular ion motion. In the mixed-cation systems, the increased cage tilting brings the hydrogen atoms of FA cations into closer contact with the iodide ions, and one might expect greater N-H···I interactions and hence the degree of hydrogen bonding to increase. Evidence for this is found in the calculated vibrational spectrum (using TRAVIS[50]) shown in Figure 4, where we focus on the region of the N-H stretching frequencies of FA^+ which appear at 3250-3550 cm^{-1}. The peak is split into two since the NH_2 group is a primary aliphatic amine and has symmetric and asymmetric (higher frequency) modes. The features of the computed vibrational spectra of FA^+ in the parent $FAPbI_3$, in-

cluding the peak splitting of ≈ 130 cm^{-1}, agree well with recent experimental data of Xie *et. al.*[38]

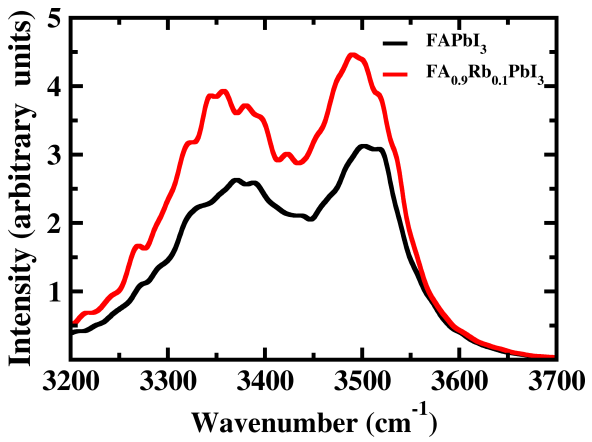

Figure 4: Vibrational spectra of $CH(NH_2)_2^+$ (FA^+) cations in $FAPbI_3$ and mixed 'A' cation, $FA_{0.9}Rb_{0.1}PbI_3$ in the region of the N-H stretching frequency. Increase in intensity and red-shift of the peaks are evident for the mixed A-site cation compound.

Crucially, as the smaller 'A' cations are incorporated into $FAPbI_3$, the N-H stretching peaks become more intense and are red-shifted (Figure 4), which is in agreement with the report by Matsui *et. al*[34] and indicates an increase in the hydrogen bond strength. This is also evidenced in a broadening of the corresponding RDF for $FA_{0.9}A_{0.1}PbI_3$ (A = Cs^+, Rb^+) in comparison to the parent $FAPbI_3$ (Figure S7 in SI), as hydrogen bond formation affects the N-H bond length in the FA^+ molecular ion.

These changes in the vibrational spectra and the RDF clearly indicate an increase in the number and strength of intermolecular N-H$\cdots$I hydrogen bonds in mixed 'A' cation perovskites over the parent $FAPbI_3$ phase. Furthermore, this feature is likely to contribute to the increased perovskite phase-stability observed in the mixed cation systems. The reduced fluctuation in the hydrogen bond distances due to locked octahedral rocking motion in these perovskites will reduce the fluctuation in the hydrogen bonding itself, and further stabilise the structure. Recent simulation studies on $MAPbI_3$[51,52] also suggest strong N-H$\cdots$I interactions between $CH_3NH_3^+$ and the Pb-I lattice.

As well as bonding effects, the 'locking' of the octahedral rotation severely impedes the motion or tumbling of the FA^+ molecular cations in the cages. Recently, several structural and computational studies have demonstrated the coupled dynamical behaviour of 'A' site cations with the surrounding inorganic framework that influences the photovoltaic performance of these halide perovskites.[48,51–57] Molecular rotations in $MAPbBr_3$ have been described as being coupled to $PbBr_6$ octahedral distortions,[48,58] while Selig *et. al.*[59] find slower cation dynamics in the mixed halide $MAPb(Br,I)_3$.

In the parent $FAPbI_3$, the FA^+ cation undergoes a tumbling motion with a time constant of 2 ps.[46] To investigate this further, we calculated the vector autocorrelation function for the FA^+ cations in all compositions. This measures the probability over time that the orientation of FA^+ cations will remain correlated with the corresponding initial orientation. Physically, it depicts how fast the organic molecular ion rotates inside the inorganic cage. The data is shown in Figure 5(a). Also shown in Figure 5(b, c) are the nitrogen density plots in which the positions of the nitrogen atoms have been stacked over time to indicate the main regions occupied.

We find three main features. First, the time constant (defined as the time taken for a 50% uncorrelation) for the parent $FAPbI_3$ is 2 ps, in excellent agreement with recent work by Weller *et al.*[46] Second, for mixed cation systems, particularly $FA_{0.9}A_{0.1}PbI_3$ (A = Cs, Rb), the time constant is more than doubled to almost 5 ps, indicating a significant reduction in the tumbling frequency of the FA^+ molecular ions. Third, for the parent $FAPbI_3$, the nitrogen density plots (Fig 5b) are essentially almost spherical indicating 3D rotation or tumbling with little restriction. This scenario is in excellent agreement with the recent study by Chen *et. al.*[60] By contrast, the nitrogen density plots for $FA_{0.9}Cs_{0.1}PbI_3$ (Fig 5c) show two distinct lobes that relate to local motion of the two NH_2^+ groups of the $CH(NH_2)_2^+$ molecular ion. This suggests that the FA^+ molecules remain mostly in a particular orientation and do not undergo full rotation nor flip through 180° during the 9 ps of simulation time.

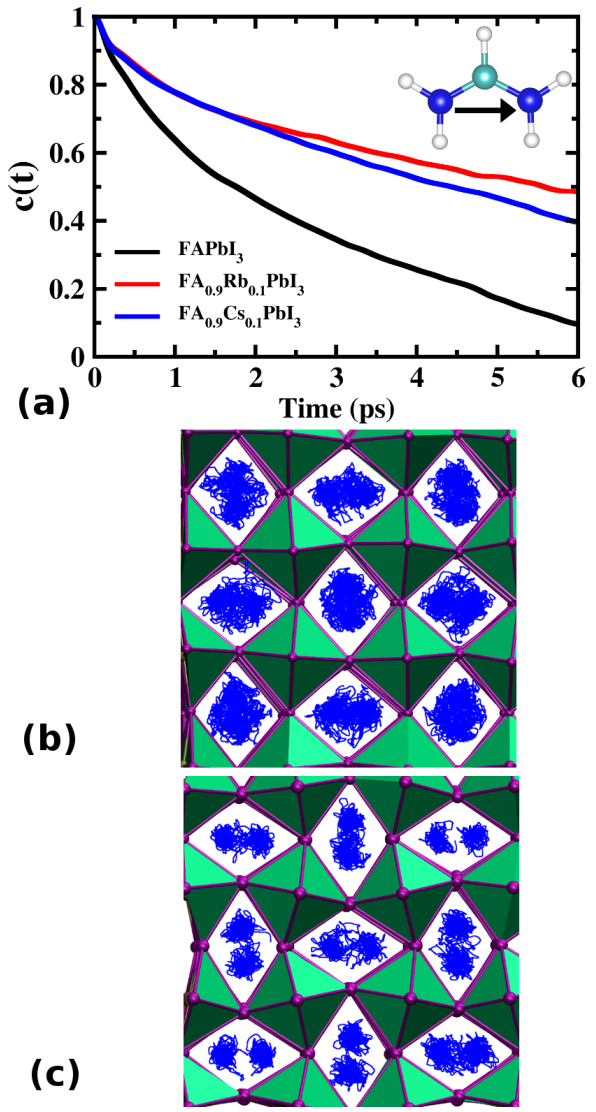

Figure 5: Dynamics of the FA^+ cation in mixed cation perovskite phases. (a) Vector autocorrelation function of FA^+ cation showing the probability of the cation remaining in its initial orientation over time. Inset shows molecular vector of FA^+ ion by an arrow. (b) Density plot showing positions of nitrogen atoms of $CH(NH_2)_2^+$ accumulated over time in $FAPbI_3$ and in (c) for $FA_{0.9}Cs_{0.1}PbI_3$.

Finally, we discuss the impact of the increased tilting and the restriction of the octahedral oscillation on the photovoltaic properties. These structural changes are significant as the electronic band gaps, relevant to photovoltaic behaviour are associated with Pb-I bond hybridization. It has been shown previously that the band-gap magnitude is sensitive to the Pb-I-Pb bond angle.[53,61] Various experimental and computational studies have found that when the Pb-I-Pb bond angle increases, the band gap also blue-shifts.[53,61] Our study indicates that the bond angle and therefore the band gap will undergo much smaller fluctuation, and result in more monochromatic light absorption profile in the mixed A-site cation perovskite systems. This reduced electronic disorder is the most likely reason for recently observed increased mobility in these mixed cation systems.[26,62] Further studies are needed to quantify this aspect as well as exploring the impact on the corresponding electronic structures.

In conclusion, we have investigated lead halide perovskites with a mixture of cation species on the A-site, which are known to show the best solar cell performance and to have higher stability against degradation. A number of structural and dynamical features that occur when $CH(NH_2)_2PbI_3$ ($FAPbI_3$) is doped with smaller cations (MA^+, Cs^+, Rb^+) on the A-site have been identified.

1. There is a contraction of the unit cell volume (of up to 2% for 10% Rb doping), which has its origin in increased tilting of the PbI_6 octahedra to compensate for the reduced space filling offered by the smaller inorganic cations.

2. The oscillation of the octahedral tilting in $FAPbI_3$ is significantly reduced with incorporation of the smaller cations, Cs^+ and Rb^+. This result indicates that the PbI_6 octahedral framework becomes 'locked' and the lattice dynamics are significantly reduced.

3. The rotational or tumbling motion of the organic molecular cations in the cages is restricted by this locking of the PbI_6 framework. For instance, the time constant of the tumbling motion of the FA^+ cations is increased from 2 ps in $FAPbI_3$ to 5 ps in both $FA_{0.9}Cs_{0.1}PbI_3$ and $FA_{0.9}Rb_{0.1}PbI_3$. There is also an increase in the hydrogen bonding type (N-H$\cdots$I) interactions between FA^+ and the Pb-I lattice in the mixed A-site cation

perovskites, which may confer greater structural stability.

The results presented here provide fundamental atomic-scale insights into the origin of the significant enhancements in solar cell performance achieved by using mixed A-site cations in lead halide perovskites and suggest design routes for further study.

Acknowledgement This work was supported by the Energy oriented Centre of Excellence (EoCoE), grant agreement number 676629, funded within the Horizon2020 framework of the European Union. MSI, PWA and CE acknowledge support from the UK Engineering and Physical Sciences Energy Materials Programme Grant (EP/K016288/1)âĂŃ and Archer HPC facilities through the Materials Chemistry Consortium (EP/L000202).

Supporting Information Available

Electronic Supplementary Information (ESI) available: detail of methods and equilibration of cubic $FAPbI_3$ in AIMD simulation, Equilibrated cell parameters and cell volumes for perovskites, time averaged structures, radial distribution function of Pb-I, Pb-N, N-H.

References

(1) Kojima, A.; Teshima, K.; Shirai, Y.; Miyasaka, T. Organometal Halide Perovskites as Visible-light Sensitizers for Photovoltaic Cells. *J. Am. Chem. Soc.* **2009**, *131*, 6050–6051.

(2) Lee, M. M.; Teuscher, J.; Miyasaka, T.; Murakami, T. N.; Snaith, H. J. Efficient Hybrid Solar Cells Based on Meso-superstructured Organometal Halide Perovskites. *Science* **2012**, *338*, 643–647.

(3) Green, M. A.; Ho-Baillie, A.; Snaith, H. J. The Emergence of Perovskite Solar Cells. *Nature Photon* **2014**, *8*, 506–514.

(4) Grätzel, M. The Light and Shade of Perovskite Solar Cells. *Nat. Mater.* **2014**, *13*, 838–842.

(5) Chen, W.; Wu, Y.; Yue, Y.; Liu, J.; Zhang, W.; Yang, X.; Chen, H.; Bi, E.; Ashraful, I.; Grätzel, M.; Han, L. Efficient and Stable Large-area Perovskite Solar Cells with Inorganic Charge Extraction Layers. *Science* **2015**, *350*, 944–948.

(6) Yang, W. S.; Noh, J. H.; Jeon, N. J.; Kim, Y. C.; Ryu, S.; Seo, J.; Seok, S. I. High-performance Photovoltaic Perovskite Layers Fabricated Through Intramolecular Exchange. *Science* **2015**, *348*, 1234–1237.

(7) Egger, D. A.; Rappe, A. M.; Kronik, L. Hybrid Organic–Inorganic Perovskites on the Move. *Acc. Chem. Res.* **2016**, *49*, 573–581.

(8) Correa-Baena, J.-P.; Abate, A.; Saliba, M.; Tress, W.; Jacobsson, T. J.; Grätzel, M.; Hagfeldt, A. The Rapid Evolution of Highly Efficient Perovskite Solar Cells. *Energy Environ. Sci.* **2017**, *10*, 710–727.

(9) Conings, B.; Drijkoningen, J.; Gauquelin, N.; Babayigit, A.; D'Haen, J.; D'Olieslaeger, L.; Ethirajan, A.; Verbeeck, J.; Manca, J.; Mosconi, E.; Angelis,; Filippo D, e.; al., Intrinsic Thermal Instability of Methylammonium Lead Trihalide Perovskite. *Adv. Energy Mater.* **2015**, *5*, 1500477.

(10) Philippe, B.; Park, B.-W.; Lindblad, R.; Oscarsson, J.; Ahmadi, S.; Johansson, E. M.; Rensmo, H. Chemical and Electronic Structure Characterization of Lead Halide Perovskites and Stability Behavior under Different Exposures - A Photoelectron Spectroscopy Investigation. *Chem. Mater.* **2015**, *27*, 1720–1731.

(11) Yang, J.; Siempelkamp, B. D.; Mosconi, E.; De Angelis, F.; Kelly, T. L. Origin of the Thermal Instability in

$CH_3NH_3PbI_3$ Thin Films Deposited on ZnO. *Chem. Mater.* **2015**, *27*, 4229–4236.

(12) Rong, Y.; Liu, L.; Mei, A.; Li, X.; Han, H. Beyond Efficiency: The Challenge of Stability in Mesoscopic Perovskite Solar Cells. *Adv. Energy Mater.* **2015**, *5*, 1501066.

(13) Berhe, T. A.; Su, W.-N.; Chen, C.-H.; Pan, C.-J.; Cheng, J.-H.; Chen, H.-M.; Tsai, M.-C.; Chen, L.-Y.; Dubale, A. A.; Hwang, B.-J. Organometal Halide Perovskite Solar Cells: Degradation and Stability. *Energy Environ. Sci.* **2016**, *9*, 323–356.

(14) Aristidou, N.; Eames, C.; Sanchez-Molina, I.; Bu, X.; Kosco, J.; Islam, M. S.; Haque, S. A. Fast Oxygen Diffusion and Iodide Defects Mediate Oxygen-induced Degradation of Perovskite Solar Cells. *Nat. Commun.* **2017**, *8*, 15218.

(15) Leguy, A. M.; Hu, Y.; Campoy-Quiles, M.; Alonso, M. I.; Weber, O. J.; Azarhoosh, P.; Van Schilfgaarde, M.; Weller, M. T.; Bein, T.; Nelson, J.; Docampo, a.; et., Reversible Hydration of $CH_3NH_3PbI_3$ in Films, Single Crystals, and Solar Cells. *Chem. Mater.* **2015**, *27*, 3397–3407.

(16) Lee, J.-W.; Seol, D.-J.; Cho, A.-N.; Park, N.-G. High-Efficiency Perovskite Solar Cells Based on the Black Polymorph of $HC(NH_2)_2PbI_3$. *Adv. Mater.* **2014**, *26*, 4991–4998.

(17) Binek, A.; Hanusch, F. C.; Docampo, P.; Bein, T. Stabilization of the Trigonal High-Temperature Phase of Formamidinium Lead Iodide. *J. Phys. Chem. Lett.* **2015**, *6*, 1249–1253.

(18) Richardson, G.; O'Kane, S. E.; Niemann, R. G.; Peltola, T. A.; Foster, J. M.; Cameron, P. J.; Walker, A. B. Can Slow-moving Ions Explain Hysteresis in the Current–voltage Curves of Perovskite Solar Cells? *Energy Environ. Sci.* **2016**, *9*, 1476–1485.

(19) Eames, C.; Frost, J. M.; Barnes, P. R.; O'regan, B. C.; Walsh, A.; Islam, M. S. Ionic Transport in Hybrid Lead Iodide Perovskite Solar Cells. *Nat. Commun.* **2015**, *6*, 7497.

(20) Snaith, H. J.; Abate, A.; Ball, J. M.; Eperon, G. E.; Leijtens, T.; Noel, N. K.; Stranks, S. D.; Wang, J. T.-W.; Wojciechowski, a.; et., Anomalous Hysteresis in Perovskite Solar Cells. *J. Phys. Chem. Lett.* **2014**, *5*, 1511–1515.

(21) Pellet, N.; Gao, P.; Gregori, G.; Yang, T.-Y.; Nazeeruddin, M. K.; Maier, J.; Grätzel, M. Mixed-organic-cation Perovskite photovoltaics for enhanced solar-light harvesting. *Angew. Chem. Int. Ed.* **2014**, *53*, 3151–3157.

(22) Jeon, N. J.; Noh, J. H.; Yang, W. S.; Kim, Y. C.; Ryu, S.; Seo, J.; Seok, S. I. Compositional Engineering of Perovskite Materials for High-performance Solar Cells. *Nature* **2015**, *517*, 476–480.

(23) Saliba, M.; Matsui, T.; Seo, J.-Y.; Domanski, K.; Correa-Baena, J.-P.; Mohammad K., N.; Zakeeruddin, S. M.; Tress, W.; Abate, A.; Hagfeldt, A.; Grätzel, M. Cesium-containing Triple Cation Perovskite Solar Cells: Improved Stability, Reproducibility and High Efficiency. *Energy Environ. Sci.* **2016**, *9*, 1989–1997.

(24) McMeekin, D. P.; Sadoughi, G.; Rehman, W.; Eperon, G. E.; Saliba, M.; Hörantner, M. T.; Haghighirad, A.; Sakai, N.; Korte, L.; Rech, B.; Johnston, M. B.; Herz, L. M.; Snaith, H. J. A Mixed-cation Lead Mixed-halide Perovskite Absorber for Tandem Solar Cells. *Science* **2016**, *351*, 151–155.

(25) Niemann, R. G.; Gouda, L.; Hu, J.; Tirosh, S.; Gottesman, R.; Cameron, P. J.; Zaban, A. Cs^+ incorporation into $CH_3NH_3PbI_3$ perovskite: substitution limit and stability enhancement. *J. Mater. Chem. A* **2016**, *4*, 17819–17827.

(26) Rehman, W.; McMeekin, D. P.; Patel, J. B.; Milot, R. L.; Johnston, M. B.; Snaith, H. J.; Herz, L. M. Photovoltaic Mixed-cation Lead Mixed-halide Perovskites: Links between Crystallinity, Photo-stability and Electronic properties. *Energy Environ. Sci.* **2017**, *10*, 361–369.

(27) Lee, J.-W.; Kim, D.-H.; Kim, H.-S.; Seo, S.-W.; Cho, S. M.; Park, N.-G. Formamidinium and Cesium Hybridization for Photo-and Moisture-stable Perovskite Solar Cell. *Adv. Energy Mater.* **2015**, *5*, 1501310.

(28) Saliba, M.; Matsui, T.; Domanski, K.; Seo, J.-Y.; Ummadisingu, A.; Zakeeruddin, S. M.; Correa-Baena, J.-P.; Tress, W. R.; Abate, A.; Hagfeldt, e.; al., Incorporation of Rubidium Cations into Perovskite Solar Cells Improves Photovoltaic Performance. *Science* **2016**, *354*.

(29) Weber, O. J.; Charles, B.; Weller, M. T. Phase Behaviour and Composition in the Formamidinium-methylammonium Hybrid Lead Iodide Perovskite Solid Solution. *J. Mater. Chem. A* **2016**, *4*, 15375–15382.

(30) Yi, C.; Luo, J.; Meloni, S.; Boziki, A.; Ashari-Astani, N.; Grätzel, C.; Zakeeruddin, S. M.; Röthlisberger, U.; Grätzel, M. Entropic Stabilization of Mixed A-cation ABX_3 Metal Halide Perovskites for High Performance Perovskite Solar Cells. *Energy Environ. Sci.* **2016**, *9*, 656–662.

(31) Qiu, W.; Ray, A.; Jaysankar, M.; Merckx, T.; Bastos, J. P.; Cheyns, D.; Gehlhaar, R.; Poortmans, J.; Heremans, P. An Interdiffusion Method for Highly Performing Cesium/Formamidinium Double Cation Perovskites. *Adv. Funct. Mater.* **2017**, *27*, 1700920.

(32) Bi, D.; Tress, W.; Dar, M. I.; Gao, P.; Luo, J.; Renevier, C.; Schenk, K.; Abate, A.; Giordano, F.; Baena, J.-P. C.; Decoppet, e.; al., Efficient Luminescent Solar Cells Based on Tailored Mixed-cation Perovskites. *Sci. Adv.* **2016**, *2*, e1501170.

(33) Soufiani, A. M.; Yang, Z.; Young, T.; Miyata, A.; Surrente, A.; Pascoe, A.; Galkowski, K.; Abdi-Jalebi, M.; Brenes, R.; Urban, J. Impact of Microstructure on the Electron–hole Interaction in Lead Halide Perovskites. *Energy Environ. Sci.* **2017**, *10*, 1358–1366.

(34) Matsui, T.; Seo, J.; Saliba, M.; Zakeeruddin, S. M.; Grätzel, M. Room Temperature Formation of Highly Crystalline Multication Perovskites for Efficient, LowÂŘ-Cost Solar Cells. *Adv. Mater.* **2017**, *29*, 1606258.

(35) Duong, T.; Wu, Y.; Shen, H.; Peng, J.; Fu, X.; Jacobs, D.; Wang, E.-C.; Kho, T. C.; Fong, K. C.; Stocks, e.; al., Rubidium Multication Perovskite with Optimized Bandgap for Perovskite-Silicon Tandem with over 26% Efficiency. *Adv. Energy Mater.* **2017**, 1700228.

(36) Syzgantseva, O. A.; Saliba, M.; Grätzel, M.; Rothlisberger, U. Stabilization of the Perovskite Phase of Formamidinium Lead Triiodide by Methylammonium, Cs, and/or Rb Doping. *J. Phys. Chem. Lett.* **2017**, *8*, 1191–1196.

(37) Li, Z.; Yang, M.; Park, J. S.; Wei, S. H.; Berry, J. J.; Zhu, K. Stabilizing Perovskite Structures by Tuning Tolerance Factor: Formation of Formamidinium and Cesium Lead Iodide Solid-State Alloys. *Chem. Mater.* **2016**, *28*, 284–292.

(38) Xie, L.-Q.; Chen, L.; Nan, Z.-A.; Lin, H.-X.; Wang, T.; Zhan, D.-P.; Yan, J.-W.; Mao, B.-W.; Tian, Z.-Q. Understanding the Cubic Phase Stabilization and Crystallization Kinetics in Mixed Cations and Halides Perovskite Single Crystals. *J. Am. Chem. Soc.* **2017**, *139*, 3320–3323.

(39) Zheng, X.; Wu, C.; Jha, S. K.; Li, Z.; Zhu, K.; Priya, S. Improved Phase Stability of Formamidinium Lead Triiodide Perovskite by Strain Relaxation. *ACS Energy Lett.* **2016**, *1*, 1014–1020.

(40) Whalley, L. D.; Frost, J. M.; Jung, Y.-K.; Walsh, A. Perspective: Theory and simulation of hybrid halide perovskites. *The Journal of Chemical Physics* **2017**, *146*, 220901.

(41) Mosconi, E.; Quarti, C.; Ivanovska, T.; Ruani, G.; De Angelis, F. Structural and Electronic Properties of Organohalide Lead Perovskites: A Combined IR-spectroscopy and Ab Initio Molecular Dynamics Investigation. *Phys. Chem. Chem. Phys.* **2014**, *16*, 16137–16144.

(42) Quarti, C.; Mosconi, E.; De Angelis, F. Structural and Electronic Properties of Organo-halide Hybrid Perovskites from Ab Initio Molecular Dynamics. *Phys. Chem. Chem. Phys.* **2015**, *17*, 9394–9409.

(43) Ivanovska, T.; Quarti, C.; Grancini, G.; Petrozza, A.; De Angelis, F.; Milani, A.; Ruani, G. Vibrational Response of Methylammonium Lead Iodide: From Cation Dynamics to Phonon–Phonon Interactions. *ChemSusChem* **2016**, *9*, 2994–3004.

(44) Quarti, C.; Mosconi, E.; Ball, J. M.; D'Innocenzo, V.; Tao, C.; Pathak, S.; Snaith, H. J.; Petrozza, A.; De Angelis, F. Structural and Optical Properties of Methylammonium Lead Iodide Across the Tetragonal to Cubic Phase Transition: Implications for Perovskite Solar Cells. *Energy Environ. Sci.* **2016**, *9*, 155–163.

(45) Brivio, F.; Frost, J. M.; Skelton, J. M.; Jackson, A. J.; Weber, O. J.; Weller, M. T.; Goni, A. R.; Leguy, A. M.; Barnes, P. R.; Walsh, A. Lattice Dynamics and Vibrational Spectra of the Orthorhombic, Tetragonal, and Cubic Phases of Methylammonium Lead Iodide. *Phys. Rev. B* **2015**, *92*, 144308.

(46) Weller, M. T.; Weber, O. J.; Frost, J. M.; Walsh, A. Cubic perovskite structure of black formamidinium lead iodide, α-$[HC(NH_2)_2]PbI_3$, at 298 K. *J. Phys. Chem. Lett.* **2015**, *6*, 3209–3212.

(47) Young, J.; Rondinelli, J. M. Octahedral Rotation Preferences in Perovskite Iodides and Bromides. *J. Phys. Chem. Lett* **2016**, *7*, 918–922.

(48) Bernasconi, A.; Malavasi, L. Direct Evidence of Permanent Octahedra Distortion in $MAPbBr_3$ Hybrid Perovskite. *ACS Energy Lett.* **2017**, *2*, 863–868.

(49) Glazer, A. The Classification of Tilted Octahedra in Perovskites. *Acta Cryst. B* **1972**, *28*, 3384–3392.

(50) Thomas, M.; Brehm, M.; Fligg, R.; Vöhringer, P.; Kirchner, B. Computing Vibrational Spectra from Ab Initio Molecular Dynamics. *Phys. Chem. Chem. Phys.* **2013**, *15*, 6608–6622.

(51) Bechtel, J. S.; Seshadri, R.; Van der Ven, A. Energy Landscape of Molecular Motion in Cubic Methylammonium Lead Iodide from First-principles. *J. Phys. Chem. C* **2016**, *120*, 12403–12410.

(52) Lee, J.-H.; Bristowe, N. C.; Lee, J. H.; Lee, S.-H.; Bristowe, P. D.; Cheetham, A. K.; Jang, H. M. Resolving the Physical Origin of Octahedral Tilting in Halide Perovskites. *Chem. Mater.* **2016**, *28*, 4259–4266.

(53) Amat, A.; Mosconi, E.; Ronca, E.; Quarti, C.; Umari, P.; Nazeeruddin, M. K.; Grätzel, M.; De Angelis, F. Cation-induced Band-gap Tuning in Organohalide Perovskites: Interplay of Spin–orbit Coupling and Octahedra Tilting. *Nano Lett.* **2014**, *14*, 3608–3616.

(54) Frost, J. M.; Butler, K. T.; Brivio, F.; Hendon, C. H.; Van Schilfgaarde, M.; Walsh, A. Atomistic Origins of High-performance in Hybrid Halide Perovskite

Solar Cells. *Nano Lett* **2014**, *14*, 2584–2590.

(55) Weller, M. T.; Weber, O. J.; Henry, P. F.; Pumpo, M. D.; Hansen, T. C. Complete Structure and Cation Orientation in the Perovskite Photovoltaic Methylammonium Lead Iodide between 100 and 352 K. *Chem. Commun.* **2015**, *51*, 3–6.

(56) Chen, T.; Foley, B. J.; Ipek, B.; Tyagi, M.; Copley, J. R.; Brown, C. M.; Choi, J. J.; Lee, S.-H. Rotational dynamics of organic cations in the $CH_3NH_3PbI_3$ perovskite. *Phys. Chem. Chem. Phys.* **2015**, *17*, 31278–31286.

(57) Kang, B.; Biswas, K. Preferential $CH_3NH_3^+$ Alignment and Octahedral Tilting Affect Charge Localization in Cubic Phase $CH_3NH_3PbI_3$. *The Journal of Physical Chemistry C* **2017**, *121*, 8319–8326.

(58) Hata, T.; Giorgi, G.; Yamashita, K.; Caddeo, C.; Mattoni, A. Development of a Classical Interatomic Potential for MAPbBr3. *J. Phys. Chem. C* **2017**, *121*, 3724–3733.

(59) Selig, O.; Sadhanala, A.; Muller, C.; Lovrincic, R.; Chen, Z.; Rezus, Y. L.; Frost, J. M.; Jansen, T. L.; Bakulin, A. A. Organic Cation Rotation and Immobilization in Pure and Mixed Methylammonium Lead-Halide Perovskites. *J. Am. Chem. Soc.* **2017**, *139*, 4068–4074.

(60) Chen, T.; Foley, B. J.; Park, C.; Brown, C. M.; Harriger, L. W.; Lee, J.; Ruff, J.; Yoon, M.; Choi, J. J.; Lee, S.-H. Entropy-driven Structural Transition and Kinetic Trapping in Formamidinium Lead Iodide Perovskite. *Sci. Adv.* **2016**, *2*, e1601650.

(61) Stoumpos, C. C.; Kanatzidis, M. G. The Renaissance of Halide Perovskites and their Evolution as Emerging Semiconductors. *Acc. Chem. Res.* **2015**, *48*, 2791–2802.

(62) Huang, Y.; Li, L.; Liu, Z.; Jiao, H.; He, Y.; Wang, X.; Zhu, R.; Wang, D.; Sun, J.; Chen, Q. The Intrinsic Properties of $FA_{(1-x)}MA_xPbI_3$ Perovskite Single Crystals. *J. Mater. Chem. A* **2017**, *5*, 8537–8544.

Graphical TOC Entry

Some journals require a graphical entry for the Table of Contents. This should be laid out "print ready" so that the sizing of the text is correct.
Inside the `tocentry` environment, the font used is Helvetica 8 pt, as required by *Journal of the American Chemical Society*.
The surrounding frame is 9 cm by 3.5 cm, which is the maximum permitted for *Journal of the American Chemical Society* graphical table of content entries. The box will not resize if the content is too big: instead it will overflow the edge of the box.
This box and the associated title will always be printed on a separate page at the end of the document.